

## A Basin-Scale Geothermal Assessment of Co-Produced Waters in Oil and Gas Fields: Uinta Basin, Utah, USA

Christian L. Hardwick, Hobie W. Willis, and Mark L. Gwynn

Utah Geological Survey, Salt Lake City, Utah  
[christianhardwick@utah.gov](mailto:christianhardwick@utah.gov)

### Keywords

*Uinta Basin, heat flow, direct use, BHT, heat conduction, co-produced water, thermal modeling*

### ABSTRACT

Co-produced waters from sedimentary basins may represent a significant geothermal resource. This study presents a regional assessment of the geothermal potential for co-produced waters from oil and gas fields of the Uinta Basin in northeastern Utah using bottom-hole temperature (BHT) and co-produced water data for 776 oil and gas wells along with available lithological information. For 136 of the wells, a BHT correction is applied using Horner and single-BHT correction methods to account for drilling-induced temperature field disturbances. From these wells, a conservative depth-dependent correction of  $+2.0^{\circ}\text{C}/\text{km}$  was derived and applied to BHTs with insufficient data for other correction methods. Corrected temperatures and typical thermal conductivities are used to calculate thermal gradients and surface heat-flow values for each well. Calculations reveal an average geothermal gradient of about  $27^{\circ}\text{C}/\text{km}$ , implying wells producing from depths greater than 2 km in the basin will likely have temperatures greater than  $65^{\circ}\text{C}$ . The average heat-flow value from wells with corrected BHTs is  $67\text{ mW}/\text{m}^2$ . These results are generally typical for gradient and heat-flow values in the Colorado Plateau. Thermal outputs are calculated using well production rates and fluid temperatures. The average thermal output is 88 kW per well with a maximum output as high as 10 MW—energy which is currently lost to waste water. The highest output wells are mostly a result of high volumetric production rates. Thermal models for the basin are created using a 3-dimensional, finite-element modeling program (COMSOL Multiphysics 4.4) and are calibrated to corrected well temperatures. Preliminary models reveal an area of approximately 16,000 km<sup>2</sup> with temperatures above  $75^{\circ}\text{C}$  at 2 km depth, and an area of 5,500 km<sup>2</sup> with temperatures above  $150^{\circ}\text{C}$  at 5 km depth. Co-produced water temperatures in 740 wells are above  $50^{\circ}\text{C}$  and may be suitable for direct-use applications such as greenhouses, space heating, and aquaculture. Binary geothermal power plants generally require a minimum temperature of  $140^{\circ}\text{C}$  to achieve acceptable efficiency and 36 wells (~5%) across the basin meet or exceed such temperatures. The thermal regime and existing infrastructure make the Uinta Basin a candidate for extensive direct-use geothermal applications and possibly binary geothermal power generation.

### Introduction

This limited, yet robust, study focuses on the geothermal energy potential of fluids co-produced from hydrocarbon plays by examining temperature data and other thermal properties from oil and gas wells in the Uinta Basin. Bottom-hole temperatures (BHT) extracted from oil and gas well logs are typically readily available, relatively inexpensive, and abundant in many study locations (Förster and Merriam, 1995; Henrikson, 2000; Henrikson and Chapman, 2002; Morgan and Scott, 2014). Heat flow and geothermal energy potential can be calculated from BHTs, associated thermal conductivities, and the consequent thermal gradient inherent in each well (Chapman and others, 1984).

There is a major problem with BHT data because the temperature of the surrounding rock is temporarily altered during the drilling process. The predominant effect is cooling that comes from the circulation of relatively cold drilling

fluids (Guyod, 1946; Bullard, 1947; Lachenbruch and Brewer, 1959; Dowdle and Cobb, 1975; Fertl and Wichmann, 1977; Harrison and others, 1983; Luheshi, 1983; Keho, 1987; Willett and Chapman, 1987; Cao and others, 1988; Deming, 1989; Deming and others, 1990; Prenskey, 1992; Förster and Merriam, 1995; Blackwell and others, 1999; Förster, 2001; Andaverde and others, 2005; Zschocke, 2005; Goutorbe and others, 2007; Edwards, 2013; Morgan and Scott, 2014). This is a major reason BHTs should be considered low precision, low reliability data that need to be carefully evaluated (Willett and Chapman, 1987). While the disturbed temperatures throughout the wellbore will eventually re-equilibrate, the time required is typically 10 to 20 times the duration of the drilling, which may mean many months for deep wells (Bullard, 1947; Steeples and Stavnes, 1982; Luheshi, 1983; Beardsmore and Cull, 2001). Since oil and gas wells will typically be in some phase of development, production, or plugged and abandoned long before the well bore has time to recover to pre-drilling temperatures, numerous methods have been developed to correct for the drilling induced temperature disturbance.

## BHT DATA

### *BHT Correction Methods*

Although a number of minor variations exist (mainly in certain assumptions that typically need to be made), Horner-type BHT corrections are commonly used in petroleum and geothermal investigations (Luheshi, 1983; Chapman and others, 1984; Hermanrud and others, 1990; Prenskey, 1992; Kutasov and Eppelbaum, 2005). The basis for these corrections is rooted in the work of Bullard (1947) and Lachenbruch and Brewer (1959), but the “Horner” name comes from the mathematically similar technique developed by Horner (1951) for examining pressure build-up in wells. Unlike the empirical methods that require only a single BHT measurement, Horner-type corrections are time-sequential, requiring BHT data from two or (preferably) more logging runs at the same depth.

Horner and Horner-derived single point correction methods of Henrikson (2000) and Henrikson and Chapman (2002) have been used with reasonable success throughout Utah and surrounding states by Allis and others (2011, 2012), Edwards (2013), Gwynn and others (2013, 2014) and Welhan and others (2014). Within the inherent limitations of all BHT correction methods (see Deming, 1989; Deming and others, 1990), we feel the Henrikson (2000) and Henrikson and Chapman (2002) methods provide reasonable estimated BHTs for the Uinta Basin.

### *BHT Data Compilation*

Two sets of BHT data for the Uinta Basin were combined in this study (figure 1). The first has data processed from 136 wells where sufficient, credible data were available to correct for the drilling-induced temperature perturbations using correction methods of Henrikson (2000) and Henrikson and Chapman (2002) compiled for the National Geothermal Data System (NGDS) by the Utah Geological Survey.

Bottom-hole temperatures for the remaining 640 wells were extracted from geophysical logs via the online Utah Division of Oil, Gas and Mining (DOG M) database. A depth-dependent correction factor specific to the Uinta Basin was derived and applied using Horner-corrected BHTs from the 136 previously corrected wells. The difference between each uncorrected BHT and the Horner-corrected temperature was calculated and the average of these values was found to be 2.0°C/km (0.11°F/100 ft).

### *Heat Flow*

In this study, corrected BHTs are combined with additional thermal data and used as inputs of the Simple Gradient and Thermal Resistance Methods for calculating one-dimensional heat-flow values following Chapman and others (1984), Keho (1987), and Henrikson (2000). The thickness of lithofacies encountered in each well in this study were taken from existing UGS data. Thermal conductivity values directly measured by

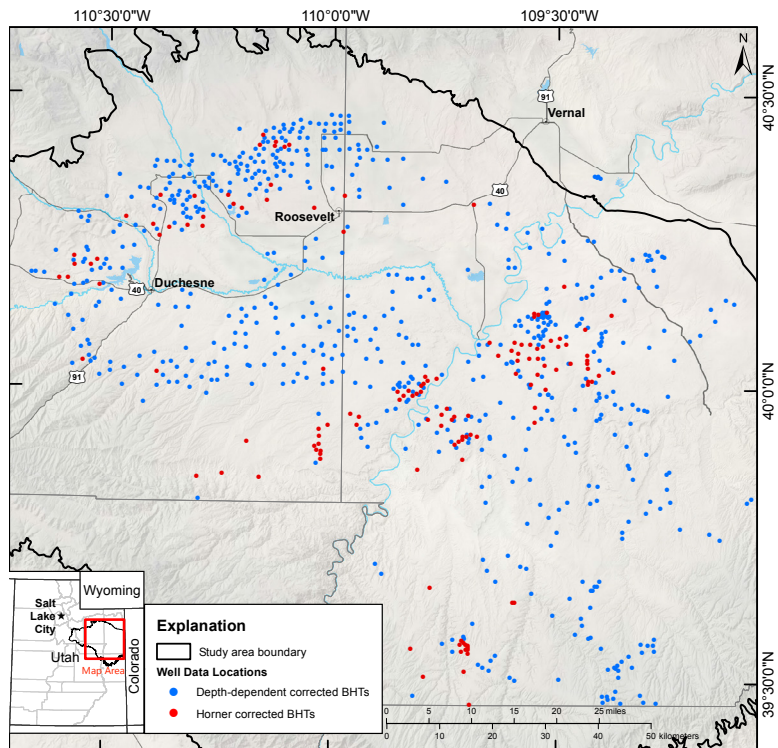


**Figure 1.** Map of Uinta Basin showing geographic distribution of wells studied.

the divided-bar method are taken from Keho (1987) and Henrikson (2000) when available. Otherwise, lithofacies were assigned a typical thermal conductivity value sourced from common industry data compiled by Beardsmore and Cull (2001). Mean annual surface ground temperature (SGT) values for each well were extrapolated from Edwards (2013). First, a thermal gradient is calculated using the Simple Gradient Method. An initial estimate of heat flow based on the Simple Gradient Method and Fourier's Law is then computed using the calculated gradient and a thickness weighted (arithmetic) mean of thermal conductivities for all stratigraphic layers within the gradient interval. With this estimate, a starting value of surface heat flow is determined and then used in the Thermal Resistance Method.

Thermal resistance is summed for all layers between the surface and BHT depth (Keho, 1987) to compute the temperature at depth (also known as bootstrapping). In this study, temperature at depth is calculated with the Thermal Resistance Method in an iterative, forward-modeling approach by adjusting the heat-flow parameter which is guided by the residual of the observed and calculated BHTs until the data are within a tolerance of 1%. The Thermal Resistance Method gives a better approximation for the final surface heat-flow value compared to the Simple Gradient Method because it incorporates all subsurface layers in the computation.

### Heat Flow Results

The mean surface heat flow for all wells studied is 67 mW/m<sup>2</sup> with a standard deviation of ±12 mW/m<sup>2</sup>. The mean thermal gradient for the data is 31°C/km with a standard deviation of ±6°C/km. A heat-flow value of 65 ±10 mW/m<sup>2</sup> and a mean geothermal gradient of 27±5°C/km were calculated after filtering anomalous wells (figures 2 and 3).

The mean surface heat flow falls within a reasonable range when compared with previous studies. Heat-flow studies by Chapman and others (1984) and Keho (1987) of 97 wells located primarily in the

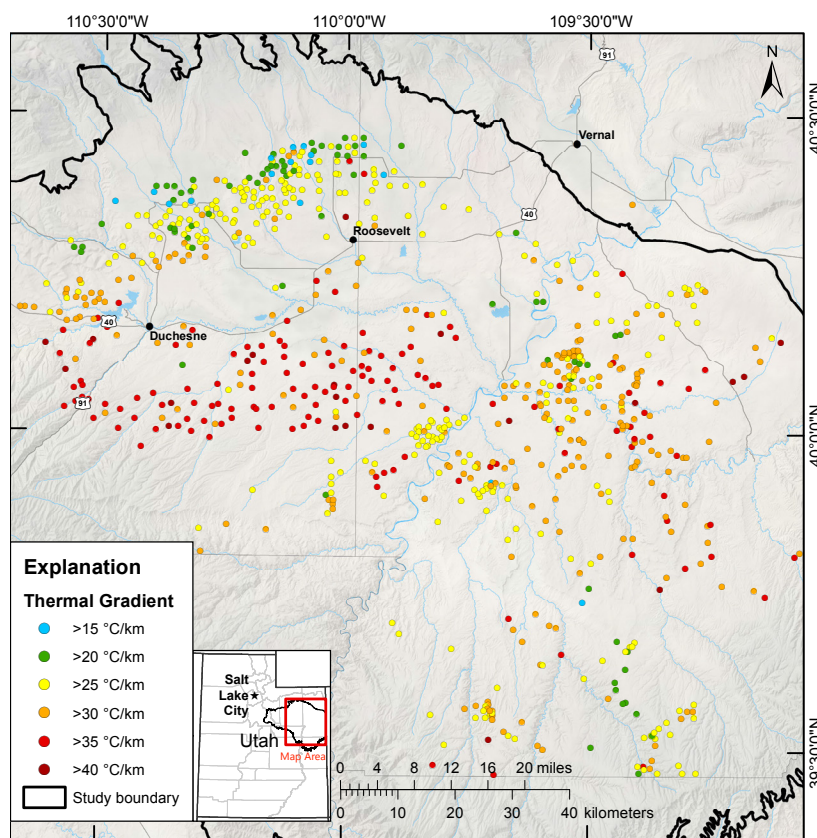


**Figure 2.** Thermal gradients of oil and gas wells. These wells, categorized by corrected BHTs, show the general trend of thermal gradients in the Uinta Basin. Gradients are slightly higher than the average of 27°C/km (1.48°F/100 ft) along the center of the basin with cooler than average gradients to the north and south. Gradients may be cooler along the northern margins due to groundwater recharge from the south flank of the Uinta Mountains.

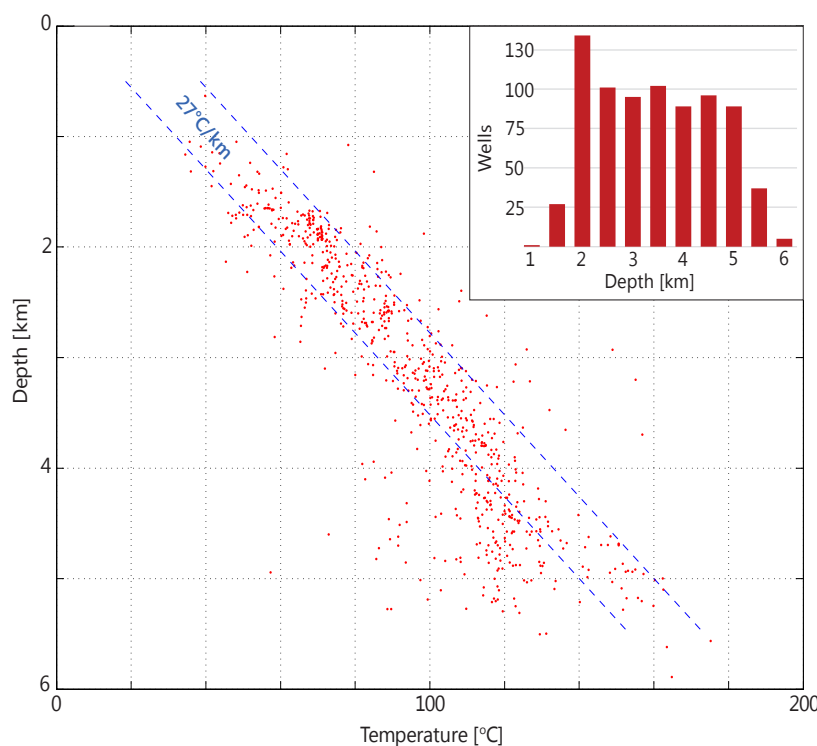


**Figure 3.** Temperatures at depth. The average thermal gradient of 27°C/km (1.48°F/100 ft) is bracketed over a range of surface temperatures. Well depth distribution shown in upper-right corner.

northwest portion of the Uinta Basin resulted in a mean heat flow of  $57 \text{ mW/m}^2 \pm 11 \text{ mW/m}^2$  from a range of 40 to  $65 \text{ mW/m}^2$ . A study of the entire Colorado Plateau by Henrikson (2000) reports a mean heat-flow value of  $62 \pm 2 \text{ mW/m}^2$  which includes around 100 heat-flow values for the Uinta Basin. Keho (1987) and Henrikson (2000) used fewer, but more accurate, BHTs in their work which may partly explain the differences. Another factor may be our use of more wells spread over a greater expanse of the Uinta Basin, a major goal of this study.

## Thermal Models

### Background Data and Methods

Building upon the observed and computed thermal data from above, we created a conductive thermal model of the Uinta Basin using COMSOL Multiphysics 4.4, a finite element method modeling program. This initial thermal model is intended to bracket the regional background heat flow so that more detailed models exploring spatial heterogeneities can be developed. The methods used by Hardwick and others (2014) to generate a similar model of the Black Rock Desert of Utah were used in this study. The model framework consists of surface topography from a 5-meter digital elevation model, a basement interface as determined by well data, and isopach maps from other UGS Uinta Basin work. In this study, a simple layer-cake model is implemented consisting of only two material layers (basement rock and basin fill material). In areas where basin-fill thickness is zero, we set the bedrock contact at 10 meters depth so that the layers are continuous without any overlap. Model layers were then smoothed within COMSOL in order to simplify the meshing and speed up computing time. We use a mean annual SGT from Edwards (2013) as the upper boundary condition and a spatially uniform basal heat flux as the lower boundary condition. Both boundary conditions are invariant with respect to time.

The range of thermal conductivities chosen for the model was determined by the measured conductivities of core and chip samples recovered from Uinta Basin wells (Keho, 1987; Henrikson, 2000) and typical values for the lithology recorded in the well logs. Thermal conductivities for the basin fill layer ( $k_1$ ) range from 2.0 to 3.0 W/mK (9 total) and for the basement rock layer ( $k_2$ ) range from 3.5 to 4.5 W/mK (9 total). Increments of 0.125 W/mK were modeled for each layer. The lower boundary condition, basal heat flow ( $q_b$ ), is uniform and a range of values from 60 to  $80 \text{ mW/m}^2$  were used (5 total). The upper and lower limits of the range for all parameters is intentionally extended slightly beyond known values as a check of the model behavior and to help define global and local minimums. A parametric sweep scheme using COMSOL results in 81 models per  $q_b$  value (405 models in total).

### Model Results and Discussion

Temperature and heat-flow residuals indicate where the thermal models correlate with the observed data. The residuals are computed from 776 observed subsurface temperature points and the respective surface heat-flow values compared to the modeled temperatures at the same locations reported as the mean, standard deviation, and maximum difference. Temperature residuals show that the models are more sensitive to changes in thermal conductivity of the basin fill

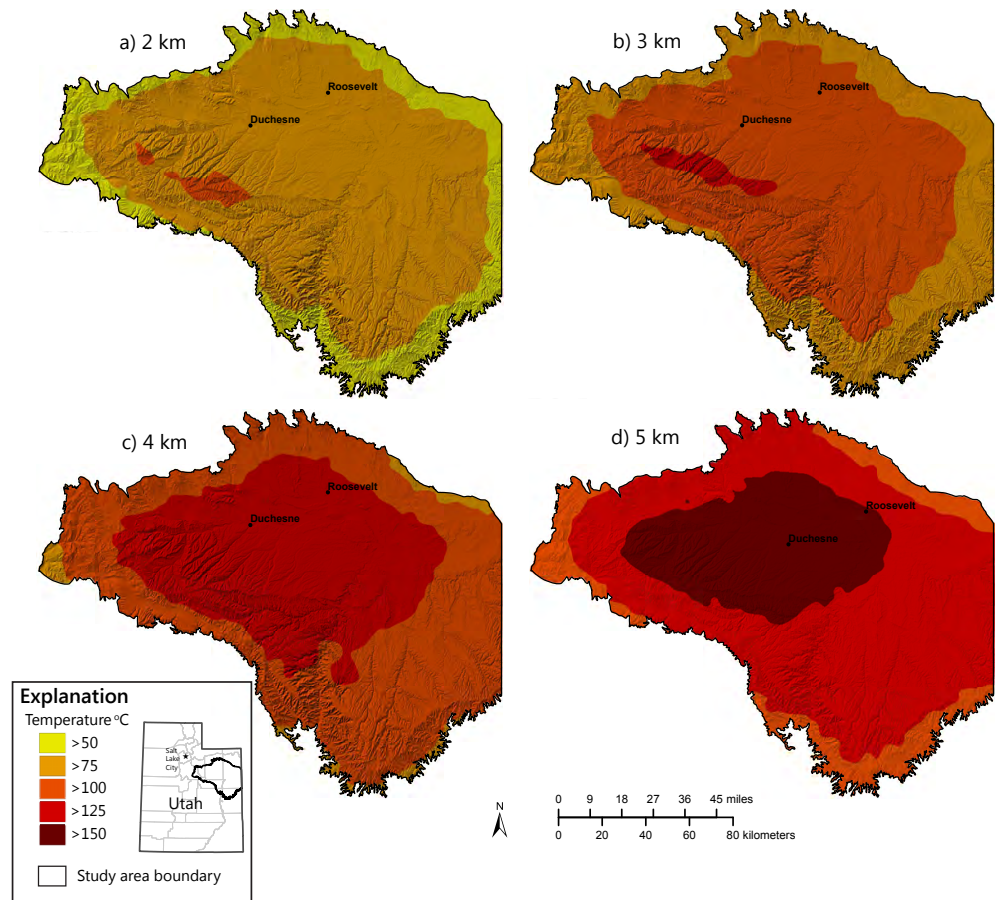


**Figure 4.** Maps of the temperature field at planes of constant elevation below the average elevation of the Uinta Basin.

rather than such changes in the basement rock. This is expected because the Uinta Basin is a deep basin (exceeding 4.5 km) and the primary effects on temperature are the insulating properties of the basin fill material. The 70 mW/m<sup>2</sup> basal heat-flow value results in the best-fit models according to temperature residuals and shows a global minimum for the  $k_1$  parameter. This overall best-fit model uses  $k_1=2.375$  and  $k_2=4.0$ , with residuals of 9.8, 9.0, and 61.9°C for mean, standard deviation, and maximum.

Heat-flow residuals vary only slightly for changes in  $k_1$  and  $k_2$  values. As with the temperature residuals, the basal flux of 70 mW/m<sup>2</sup> contains the best-fit model as well as the lowest model residuals for all combinations of  $k_1$  and  $k_2$  compared to other basal-flux values. The best-fit basal flux model for heat-flow residuals has the same  $k_1$  and  $k_2$  values as the best temperature residual model. The heat-flow residuals are 8.0, 7.0, and 46.0 mW/m<sup>2</sup> for the mean, standard deviation, and maximum difference.

Temperature slices shown in figure 4 from the Uinta Basin thermal model are produced at depths of 2, 3, 4, and 5 km below the average surface elevation of the basin. For an area of 16,000 km<sup>2</sup> we find that temperatures are generally greater than 75°C at a depth of 2 km and in some areas exceed 100°C. In this assessment, the calculated minimum temperature required for direct use applications (greenhouses, etc.) is 50°C which is met at 2 km depth in the entire basin model. Modeled temperatures reach 150°C at a depth of 5 km below the basin which exceeds the minimum temperature of 140 °C required for binary geothermal power production.

The modeled surface heat flow in the Uinta Basin ranges from 50 to over 80 mW/m<sup>2</sup> (figure 5). Surface heat-flow values are generally highest in the mountains and lowest in the valleys. Due to the refraction of heat flow along the basin/basement interface we expect basement bedrock values to exceed the uniform basal flux of 70 mW/m<sup>2</sup>. This is observed in the model along the margins of the Uinta Basin where basin-fill thickness is thin and basement is at or near the surface. Average surface heat flow for the Uinta Basin using the thermal resistance method is 67 mW/m<sup>2</sup> which agrees reasonably with the best-fit thermal model and suggests that the thermal regime of the basin may be primarily conductive.

When comparing the 3D model to the 1D calculations there are some key differences to point out. Since the primary intention of the initial 3D model is to constrain the background regional heat flow, disparities are expected when examined against the 1D values. These differences typically can be due to the result of advective or convective heat transport rather than conduction. We find that differences are most prominent at the northern end of the Uinta Basin where the thermal model over predicts the 1D values by up to 30 mW/m<sup>2</sup> or more. One proposed explanation for this difference is that regional groundwater flow is flushing the heat (cooling the host rock) via recharge pathways originating in the Uinta Mountains and moving southward into the basin. This hypothesis of groundwater flow is also suggested by a number of saline water studies of the Uinta Basin (Howells and others, 1987; Freethey, 1992; Glover, 1996; Zhang and others, 2009; Anderson and others, 2012) in order to explain the great depth to the base of the saline water in the northern Uinta Basin. We find that this deep trend is coincident with low heat-flow values (figure 6) and most likely a cause and effect relation. An east-west trend of under predicted heat flow is observed through the central part of the basin where model results are lower than 1D values by 15 mW/m<sup>2</sup> on average. This trend aligns with the Duchesne

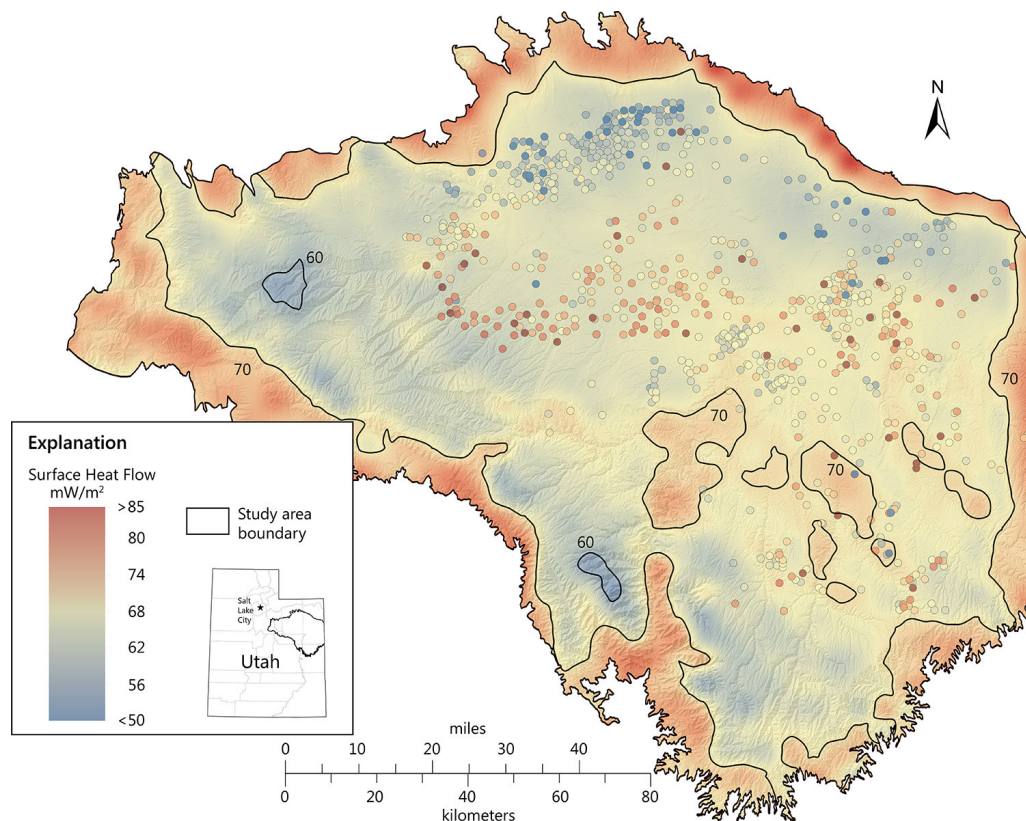
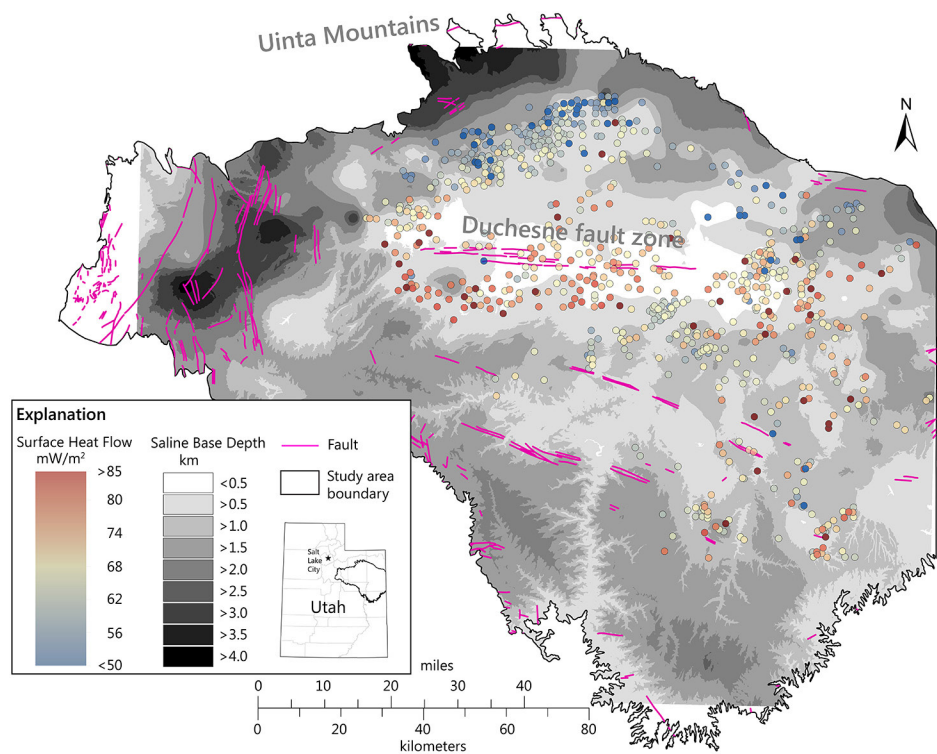


**Figure 5.** Surface heat flow from Uinta Basin thermal model and corrected well data (symbols colored according to heat-flow values). Black lines are contours of heat flow in 10 mW/m<sup>2</sup> intervals.

**Figure 6.** Map of depth in km to the base of the moderately saline water (data from Anderson and others, 2012) in the Uinta Basin. Well locations and calculated heat-flow values (symbols colored according to heat-flow values) are shown. Magenta lines are faults. A noticeable spatial correlation between the depths to the base of the moderately saline water and heat flow can be observed. Heat-flow values are lower in the northern area where the base to the saline water is deep and heat-flow values are higher in the central part of the basin where the base to the saline water is shallow.

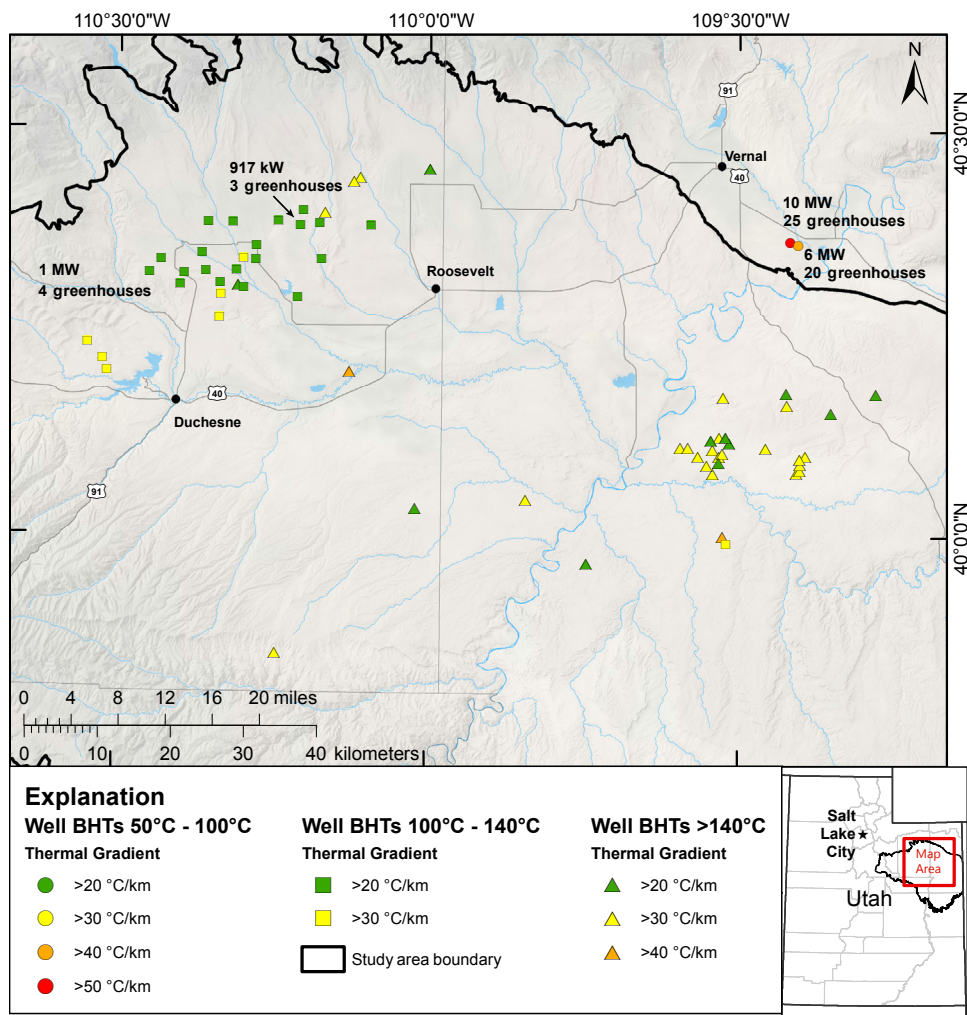


fault zone as well as a shallow trend of the moderately saline fluid base. The shallow base is thought to be related to the upward mobility of fluids enabled by the fault-and-fracture system (among other factors) according to Anderson and others (2012). Heat transport within these upward moving fluids could explain the elevated heat flow in the central part of the basin, coincident with the Duchesne fault zone. In order to facilitate a more in-depth study of the Uinta Basin, revised versions of the 3D thermal models should incorporate fluid flow components to better address the effects of the groundwater flow hypotheses.

### Geothermal Resource Potential

This study shows that co-produced fluids from oil and gas wells within the Uinta Basin may represent a significant, yet

**Figure 7.** Map of wells co-producing water at a sufficient volume to support at least one 468 m<sup>2</sup> (5,037 sq ft) greenhouse (square symbol, indicated when more than three can be supported) and wells meeting required temperature threshold (> 140°C) for binary power generation (triangles). The potential is greatest for wells in the Ashley Valley field near Vernal, in the northwest quadrant of the map, due to high volumetric output of co-produced fluid.



unused, geothermal resource. The mean thermal gradient of 27°C/km for the Uinta Basin implies that any well deeper than 2 km could have a fluid temperature of about 65°C when using a mean annual SGT of 11°C. This temperature is well above the minimum threshold required for heated fluids to be used in direct-use applications such as aquaculture, greenhouses, and space heating (Boyd, 2008). Since the average depth of wells in this study is 3 km, higher temperatures can be expected from the majority of producing wells.

Fluid production volumes from Uinta Basin wells have been averaged using available data, which, in many cases, represents the entire production period for a given well. With documented flow and temperature values we can calculate the heat content and thermal output of each well. Applying this calculation to our Uinta Basin dataset results in an average thermal output of 88 kW, but a maximum output of up to 10 MW was calculated for wells with exceptionally high volumes of produced fluids. Of the wells studied, 587 of the 776 fall in a range of 25 to 100 kW of thermal output.

Resource fluid temperatures between 120°C and 150°C are suitable for binary-cycle geothermal power plants (Blackett and others, 2004). Temperatures above 120°C are found in 127 wells in our dataset. However, useable heat content is limited by the temperature difference between the surface and the production depth. In addition, the efficiency of existing geothermal power plants demonstrates that a resource temperature at or above 140°C is preferred (Blackett and others, 2004). Such temperatures are observed in 36 wells in this study (figure 7).

Alternatively, produced fluids could be used for direct-use geothermal applications such as greenhouse heating. Greenhouse heating requirements are highly variable depending on several factors including, but not limited to, greenhouse size/volume, structural materials, heat delivery methods, crop requirements, and weather (Boyd, 2008). A fiberglass-plastic style greenhouse covering an area of 468 m<sup>2</sup> would require 51 kW of power to maintain an internal temperature of 21°C with a mean external temperature of 10°C. Additional design parameters from Boyd (2008) and Lund (2011) reveal that a single well must produce 3 to 5 m<sup>3</sup>/min of >50°C fluids to sustain the greenhouse described above. Minimum temperatures are found in 740 wells in our dataset, and 29 of these also meet the flow requirements of our example greenhouse. These wells could support a total of 86 greenhouses (figure 7). Regardless of volumetric production, the high number of existing wells producing fluids above 50°C make direct-use geothermal applications (i.e., greenhouses) in the Uinta Basin an attractive option.

## Conclusions

This geothermal assessment of the Uinta Basin presents encouraging results related to geothermal potential in a number of ways. With a well-distributed sampling of thermal data in the Uinta Basin, we are able to identify key thermal characteristics that are important to geothermal prospecting and the possibility of future development. Average background heat flow of 67 mW/m<sup>2</sup> and an average geothermal gradient of 27°C/km result in adequate temperatures (>50°C) at depths greater than 2 km for direct use applications such as greenhouses. This is important because of the large number of wells that are deeper than 2 km and the pre-existing well infrastructure (significant cost savings for development) in the basin. Preliminary thermal models of the Uinta Basin give some support to existing interpretations that the thermal regime is primarily conductive with the exception of groundwater flushing from the Uinta Mountains and upward flow along faults in the central basin. A conductive regime implies that the thermal aspects, intra-basin systems and responses are more predictable and likely are uniformly spread across the basin, resulting in a larger geothermal prospect. Future models incorporating basin-scale fluid flow will provide better estimates of the resource potential within the basin. From this small subset of Uinta Basin well data, we find 740 wells meet the temperature requirement of 50°C for direct-use applications and 36 wells meet the temperature requirement of 140°C for binary geothermal power production. The average thermal output per well is 88 kW and maximum output is as high as 10 MW. For each well, produced oil volumes decrease and co-produced fluids increase and the door opens to even more geothermal resource that could be used locally.

## Acknowledgements

Funding for this ongoing research is provided by Research Partnership to Secure Energy for America (RPSEA), contract number 11123-08. Additional funding was provided by the Utah Geological Survey. We kindly thank the reviewers for providing constructive criticism and valuable editing to improve the overall quality of this manuscript.

## References

- Allis, R., Blackett, R., Gwynn, M., Hardwick, C., Moore, J.N., Morgan, C., Schelling, D., and Sprinkel, D., 2012, Stratigraphic reservoirs in the Great Basin—the bridge to enhanced geothermal systems in the U.S.: Transactions, Geothermal Resources Council, v. 36, p. 351–357.
- Allis, R., Moore, J., Blackett, B., Gwynn, M., Kirby, S., and Sprinkel, D., 2011, The potential for basin-centered geothermal resources in the Great Basin: Transactions, Geothermal Resources Council, v. 35, p. 683–688.

- Andaverde, J., Verma, S.P., and Santoyo, E., 2005, Uncertainty estimates of static formation temperatures in boreholes and evaluation of regression models: *Geophysics Journal International*, v. 160, p. 1112–1122.
- Anderson, P. B., Vanden Berg, M. D., Carney, S., Morgan, C., and Heuscher, S., 2012, Moderately saline groundwater in the Uinta Basin, Utah: *Utah Geological Survey Special Study 144*, 30 p.
- Beardsmore, G.R., and Cull, J.P., 2001, *Crustal heat flow—a guide to measurement and modeling*: Cambridge, Cambridge University Press, 334 p.
- Blackett, R.E., Sowards, G.M., and Trimmer, E., 2004, Utah’s high temperature geothermal resource potential—analysis of selected sites: *Utah Geological Survey Open File Report*, 124 p.
- Blackwell, D.D., Beardsmore, G.R., Nishimori, R.K., and McMullen, R.J., Jr., 1999, High resolution temperature logs in a petroleum setting—examples and applications, *in*, Förster, A., and Merriam, D.F., editors, *Geothermics in basin analysis*: New York, Plenum Press, p. 1-34.
- Boyd, T., 2008, *Geothermal greenhouse information package*: Oregon Institute of Technology, 287 p.
- Bullard, E.C., 1947, The time necessary for a borehole to attain temperature equilibrium: *Monthly Notices, Royal Astronomical Society, Geophysical Supplement*, v. 5, no. 5, p. 127-130.
- Cao, S., Lerche, I., and Hermanrud, C., 1988, Formation temperature estimation by inversion of borehole measurements: *Geophysics*, v. 53, p. 979–988.
- Chapman, D.S., Keho, T.H., Bauer, M.S., and Picard, D.M., 1984, Heat flow in the Uinta Basin determined from bottom hole temperature (BHT) data: *Geophysics*, v. 49, no. 4, p. 453–466.
- Deming, D., 1989, Application of bottom-hole temperature corrections in geothermal studies: *Geothermics*, v. 18, no. 5/6, p. 775–786.
- Deming, D., Nunn, J.A., Jones, S., and Chapman, D.S., 1990, Some problems in thermal history studies, *in* Nuccio, V.F. and Barker, C.E., editors, *Applications of thermal maturity studies to energy exploration, 1990: Rocky Mountain Section, Society for Sedimentary Geology*, p. 61-80.
- Dowdle, W.L., and Cobb, W.M., 1975, Static formation temperature from well logs—an empirical method: *Journal of Petroleum Technology*, v. 27, no. 11, p. 129–135.
- Edwards, M.C., 2013, *Geothermal resource assessment of the Basin and Range Province in western Utah*: Salt Lake City, University of Utah, M.S. thesis, 133 p.
- Fertl, W.H., and Wichmann, P.A., 1977, How to determine static BHT from well log data: *World Oil*, v. 184, p. 105–106.
- Förster, A., 2001, Analysis of borehole temperature data in the Northeast German Basin—continuous logs versus bottom-hole temperatures: *Petroleum Geoscience*, v. 7, p. 241–254.
- Förster, A., and Merriam, D.F., 1995, A bottom-hole temperature analysis in the American Midcontinent (Kansas)—implications to the applicability of BHTs in geothermal studies, *in* *World Geothermal Congress 1995, Firenze, Italy, May 18–31, 1995, Proceedings: International Geothermal Association*, v. 2, p. 777-782.
- Freethy, G.W., 1992, Maps summarizing geohydrologic information in an area of salt-water disposal, eastern Altamont-Bluebell Petroleum Field, Uinta Basin, Utah: *U.S. Geological Survey Water Resource Investigation Report WRIR 92-4043*, 2 plates.
- Glover, K.R., 1996, Ground-water flow in the Duchesne River–Uinta aquifer in the Uinta basin, Utah and Colorado: *U.S. Geological Survey Water Resource Investigation Report 92-4161*, p. 24.
- Goutorbe, B., Lucazeau, F., and Bonneville, A., 2007, Comparison of several BHT correction methods—a case study on an Australian data set: *Geophysics Journal International*, v. 170, no. 2, p. 913–922.
- Guyod, H., 1946, Temperature well logging [a seven-part series]: *Oil Weekly*, v. 123, no. 8–11, (October 21, 28; November 4, 11), v. 124, no. 1–3 (December 2, 9, 16).
- Gwynn M., Allis, R., Blackett, R., and Hardwick, C., 2013, New geothermal resource delineated beneath Black Rock Desert, Utah, *in* *Thirty-Eighth Workshop on Geothermal Reservoir Engineering, Stanford, California, February 11–13, 2013, Proceedings: Stanford University, SGP-TR-198*, 9 p.
- Gwynn, M., Allis, R., Sprinkel, D., Blackett, R., and Hardwick, C., 2014, Geothermal potential in the basins of northeastern Nevada: *Transactions, Geothermal Resources Council*, v. 38, p. 1029–1039.
- Hardwick, C. L., Kirby, S., and Gwynn, M., 2014, Geothermal prospecting in Utah—a new thermal model of the Black Rock Desert: *Transaction, Geothermal Resources Council*, v. 38, p. 1041-1045.
- Harrison, W.E., Luza, K.V., Prater, M.L., and Cheung, P.K., 1983, *Geothermal resource assessment in Oklahoma*: Oklahoma Geological Survey Special Publication 83–1, 42 p.
- Henrikson, A. 2000, *Heat flow determination from oil and gas wells in the Colorado Plateau and Basin and Range of Utah*: Salt Lake City, University of Utah, M.S. thesis, 69 p.
- Henrikson, A., and Chapman, D.S., 2002, *Terrestrial heat flow in Utah*: Salt Lake City, University of Utah, unpublished report, 47 p.
- Hermanrud, C., Cao, S., and Lerche, I., 1990, Estimates of virgin rock temperature derived from BHT measurements—bias and error: *Geophysics*, v. 55, no. 7, p. 924–931.
- Horner, D.R., 1951, Pressure build-up in wells *in* 3<sup>rd</sup> World Petroleum Congress, The Hague, the Netherlands, May 28–June 6, 1951, *Proceedings: World Petroleum Congress*, p. 25–43.
- Howells, L., Longson, M.S., and Hunt, G.L., 1987, Base of moderately saline ground water in the Uinta basin, Utah, with an introductory section describing the methods used in determining its position: *Utah Department of Natural Resources Technical Publication 92*, 59 p., 2 plates, scale 1:250,000. Also available as: *U.S. Geological Survey Open-File Report 87-394*.
- Keho, T.H., 1987, *Heat flow in the Uinta Basin determined from bottom hole temperature (BHT) data*: Salt Lake City, University of Utah, M.S. thesis, 99 p.

- Kutasov, I.M., and Eppelbaum, L.V., 2005, An improved Horner method for determination of formation temperature, *in* World Geothermal Congress 2005, Antalya, Turkey, April 24–29, 2005, Proceedings: International Geothermal Association, 8 p.
- Lachenbruch, A.H., and Brewer, M.C., 1959, Dissipation of the temperature effect of drilling a well in Arctic Alaska: U.S. Geological Survey Bulletin 1083-C, p. 73–109.
- Luheshi, M.N., 1983, Estimation of formation temperature from borehole measurements: *Geophysical Journal*, Royal Astronomical Society, v. 74, p. 747–776.
- Lund, J.W., 2011, Development of Direct-Use Projects, *in* Thirty-Sixth Workshop on Geothermal Reservoir Engineering, Stanford, California, January 31–February 2, 2011, Proceedings: Stanford University, SGP-TR-191, 11 p.
- Morgan, P., and Scott, B., 2011, Bottom-hole temperatures data from the Piceance Basin, Colorado—indications for prospective sedimentary basin EGS resources: *Transactions, Geothermal Resources Council*, v. 35, p. 477–485.
- Morgan, P., and Scott, P., 2014, New geothermal-gradient maps for Colorado’s sedimentary basins: *Transactions, Geothermal Resources Council*, v. 38, p. 155–162.
- Prensky, S., 1992, Temperature measurements in boreholes—an overview of engineering and scientific applications: *The Log Analyst*, v. 33, no. 3, p. 313–333.
- Steeple, D.W., and Stavnes, S.A., 1982, Assessment of geothermal resources of Kansas: U.S. Department of Energy Final Report DOE/ET/27204-T1-Vol. 1-Sect.1, 59 p.
- Welhan, J.A., Gwynn, M.L., Payne, S., McCurry, M.O., Plummer, M., and Wood, T., 2014, The Blackfoot Volcanic Field, Southeast Idaho—a hidden high-temperature geothermal resource in the Idaho Thrust Belt, *in* Thirty-Ninth Workshop on Geothermal Reservoir Engineering, Stanford, California, February 24–26, 2014, Proceedings: Stanford University, SGP-TR-202, 13 p.
- Willett, S.D., and Chapman, D.S., 1987, Analysis of temperatures and thermal processes in the Uinta Basin, *in* Beaumont, C., and Tankard, A.J., editors, *Sedimentary basins and basin-forming mechanisms: Canadian Society of Petroleum Geologists Memoir No. 12*, p. 227–261.
- Zhang, Y., Gable, C.W., Zivoloski, G.A., and Walter, L.M., 2009, Hydrogeochemistry and gas compositions of the Uinta Basin—a regional-scale overview: *American Association of Petroleum Geologist Bulletin*, v. 93, no. 8, p. 1087–1118.
- Zschocke, A., 2005, Correction of non-equilibrated temperature logs and implications for geothermal investigations: *Journal of Geophysics and Engineering*, v. 2, p. 364–371.

